3D full waveform inversion for ocean-bottom seismic data based on the acoustic-elastic coupled wave-equation system

Jian Cao, Romain Brossier, Ludovic Métivier

3D full waveform inversion for ocean-bottom seismic data based on the acoustic-elastic coupled wave-equation system

J. Cao[1*], R. Brossier[1], L. Métivier[1,2]

[1] Univ. Grenoble Alpes, ISTerre, F-38058 Grenoble, France
[2] CNRS, Univ. Grenoble Alpes, LJK, F-38058 Grenoble, France

Thursday 14th January, 2021

Main objectives

This study considers the 3D full waveform inversion (FWI) for ocean-bottom seismic data within the framework of elastic approximation for the subsurface. The methodology of FWI in the acoustic-elastic coupled wave-equation system is developed to fit and invert the elastic effects captured by the ocean-bottom acquisition, which allows for the S-wave velocity reconstruction and resolution enhancement in the marine seismic exploration.

New aspects covered

Based on the adjoint-state method, the gradient kernels of FWI in the acoustic-elastic coupled wave-equation system are constructed efficiently in a hybrid way, which provides the possibility of inverting the elastic properties of the subsurface. The application of acoustic-elastic coupled FWI to the ocean-bottom seismic data is demonstrated to yield superior velocity reconstructions compared to the conventional streamer acquisition, especially for the usage of 3C displacement data.

Summary (200 words)

Ocean-bottom seismic acquisition is attractive in the exploration of complex deep-water environments due to its source-receiver decoupling, which makes it possible to get a wide-azimuth coverage and long source-receiver distance to significantly improve the illumination at depth. However, such acquisition systems also provide information on the elastic properties of the subsurface by recording the displacement on the seabed with 3C geophones. This information is mostly overlooked up to now, while reconstructing jointly P-wave and S-wave velocity models would significantly improve the subsurface characterization. Achieving such a high-resolution multi-parameter reconstruction requires the design of an efficient 3D fluid-solid coupled inversion engine. The purpose of this study is to present such a tool, based on an acoustic-elastic coupled wave-equation system and a spectral-element discretization in space. The method is illustrated on a bilayered 2D model and a 3D extended Marmousi model, to show how P-wave and S-wave velocity models can be inferred from the data, and the resolution improvement obtained from the reconstruction of the S-wave velocity model.

Introduction

As the marine seismic exploration moves to complex deep-water geologic environments, ocean-bottom seismic acquisition (either ocean-bottom cables (OBC) or ocean-bottom nodes (OBN)) begins to be used as an effective technology for imaging quality enhancement and risk reduction. Compared with the streamer acquisition, this acquisition has the advantages of decoupling the sources from receivers to achieve a wide-azimuth coverage and long source-receiver distance for the illumination improvement at depth, and providing more subsurface information through hydrophones in the water and 3C geophones on the seabed which can record more elastic effects for S-wave velocity reconstruction (Maver, 2011).

Full waveform inversion (FWI) is a powerful technique to extract high-resolution quantitative physical parameters of the subsurface by fitting the full information of seismic data (Virieux and Operto, 2009). In marine exploration, most cases are performed in the acoustic approximation using the pressure wavefield only. However, this implies that the solid Earth is viewed as a fluid, ignoring its elastic properties. Furthermore, to make good use of the recorded elastic effects from 3C geophones and better mimic the true physics, the FWI based on elastic approximation needs to be applied. For reducing computational cost and memory requirement, we consider only using the elastic wave equation in the subsurface and the wave propagation in the above water layer is still modeled by the acoustic wave equation. Consequently, the forward problem in the fluid-solid coupled medium is described by an acoustic-elastic coupled wave-equation system, and the corresponding methodology of FWI gradient computation is developed on it by using the adjoint-state method (Plessix, 2006). The proposed 3D acoustic-elastic coupled inversion engine adopts a two-formulation hybrid approach in the gradient computation, which makes it possible to re-exploit the forward modeling engine for the solution of the adjoint system. Numerical tests of this acoustic-elastic coupled inversion engine is performed on a bilayered 2D model and a 3D extended Marmousi II model, in which the combined acoustic and elastic gradient kernels are illustrated and the reconstructed models using different datasets are compared.

Methodology

In the forward problem, the acoustic-elastic coupled wave-equation system is commonly formulated in terms of fluid potential φ and solid displacement $\mathbf{u}_s$ (Chaljub and Valette, 2004; Peter et al., 2011):

$$\begin{aligned}
&\tfrac{1}{\kappa}\ddot{\varphi} - \nabla\cdot\left(\tfrac{1}{\rho_f}\nabla\varphi\right) = \tfrac{1}{\kappa}\iint -P_f dt dt, && \text{in } \Omega_f,\\
&\rho_s\ddot{\mathbf{u}}_s = \nabla\cdot\boldsymbol{\sigma} + \mathbf{f}_s, \quad \boldsymbol{\sigma} = \mathbf{C}:\boldsymbol{\varepsilon}, && \text{in } \Omega_s,\\
&\mathbf{u}_s\cdot\mathbf{n} = \tfrac{1}{\rho_f}\nabla\varphi\cdot\mathbf{n}, \quad \boldsymbol{\sigma}_s\cdot\mathbf{n} = \ddot{\varphi}\mathbf{n}, && \text{on } \Gamma_{fs},
\end{aligned} \tag{1}$$

where Ω_f and Ω_s denote the fluid and solid regions, respectively, Γ_{fs} denotes the fluid-solid interface with the unit normal vector $\mathbf{n}$, and $\boldsymbol{\sigma}$ and $\boldsymbol{\varepsilon}$ are the stress and strain tensors in the solid region. The material parameters of the fluid are the density ρ_f and bulk modulus κ, and for the solid are the density ρ_s and elastic stiffness tensor $\mathbf{C}$. The source term can be applied in the fluid region in terms of pressure P_f or in the solid region as body force $\mathbf{f}_s$. For simplicity, we refer to Eq. (1) as the $\varphi-\mathbf{u}_s$ formulation.

To apply the FWI technique on the ocean-bottom seismic data, a L_2 misfit function can be defined as

$$J(\mathbf{m}) = \tfrac{1}{2}\sum_{s,r}\left(\|\mathbf{S}_{s,r}\mathbf{d}_P^{cal} - \mathbf{d}_P^{obs}\|^2 + \|\mathbf{S}_{s,r}\mathbf{d}_{\mathbf{u}}^{cal} - \mathbf{d}_{\mathbf{u}}^{obs}\|^2\right), \tag{2}$$

where $\mathbf{S}_{s,r}$ is the restriction operator onto the position of receiver r for a specific shot s, $\mathbf{d}_P^{cal}$ and $\mathbf{d}_{\mathbf{u}}^{cal}$ are the synthetic pressure data and 3C displacement data, and $\mathbf{d}_P^{obs}$ and $\mathbf{d}_{\mathbf{u}}^{obs}$ are the observed pressure data and 3C displacement data. In the minimization of Eq. (2), the forward equation system needs to serve as the constraint conditions. Based on the adjoint-state method, the gradient of Eq. (2) is computed through the cross-correlation of forward wavefields and adjoint wavefields. If we derive the adjoint system from the $\varphi-\mathbf{u}_s$ formulation, the resulting coupling conditions would require to modify the wave propagation engine. However, through reformulating the acoustic-elastic coupled wave-equation system using the pressure P in the acoustic wave equation, we can obtain an adjoint system which has a similar structure as Eq. (1)

$$\begin{aligned}
&\tfrac{1}{\kappa}\ddot{\mu} - \nabla\cdot\left(\tfrac{1}{\rho_f}\nabla\mu\right) = \sum_{s,r}\mathbf{S}_{s,r}^T\left(\mathbf{S}_{s,r}\mathbf{d}_P^{cal} - \mathbf{d}_P^{obs}\right), && \text{in } \Omega_f,\\
&\rho_s\ddot{\boldsymbol{\lambda}} = \nabla\cdot\mathbf{T} + \sum_{s,r}\mathbf{S}_{s,r}^T\left(\mathbf{S}_{s,r}\mathbf{d}_{\mathbf{u}}^{cal} - \mathbf{d}_{\mathbf{u}}^{obs}\right), \quad \mathbf{T} = \mathbf{C}:\nabla\boldsymbol{\lambda}, && \text{in } \Omega_s,\\
&\boldsymbol{\lambda}\cdot\mathbf{n} = \tfrac{1}{\rho_f}\nabla\mu\cdot\mathbf{n}, \qquad \mathbf{T}\cdot\mathbf{n} = \ddot{\mu}\mathbf{n} && \text{on } \Gamma_{fs}.
\end{aligned} \tag{3}$$

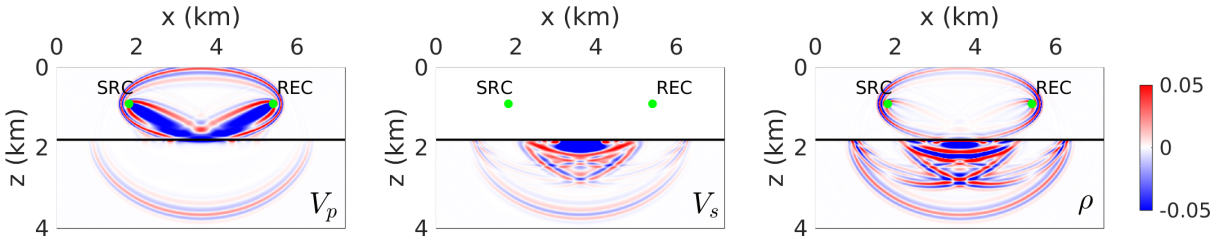

Figure 1: Gradient kernels of P-wave velocity (V_p), S-wave velocity (V_s) and density (ρ) in the acoustic-elastic coupled FWI. The source (SRC) and receiver (REC) denoted by green dots are both in the fluid region.

where μ and $\boldsymbol{\lambda}$ are the adjoint wavefields of the pressure P and solid displacement $\mathbf{u}$, respectively. This expression implies that the forward modeling engine for Eq. (1) can also be used for the solution of the adjoint system (Eq. (3)). According to the gradient expressions of density ρ and bulk modulus κ in the fluid region

$$\frac{\partial J(\mathbf{m})}{\partial \rho} = \left(\nabla\tilde{\mu}, \frac{1}{\rho^2}\nabla P\right)_{\Omega_f,t}, \qquad \frac{\partial J(\mathbf{m})}{\partial \kappa} = \left(\tilde{\mu}, \frac{1}{\kappa^2}\ddot{P},\right)_{\Omega_f,t}, \tag{4}$$

and the gradient expressions of density ρ and elastic stiffness tensor $\mathbf{C}$ in the solid region

$$\frac{\partial J(\mathbf{m})}{\partial \rho} = -(\boldsymbol{\lambda}, \ddot{\mathbf{u}})_{\Omega_s,t}, \qquad \frac{\partial J(\mathbf{m})}{\partial C_{ijkl}} = -\left(\nabla\boldsymbol{\lambda}, \frac{\partial \mathbf{C}}{\partial C_{ijkl}} :: \nabla\mathbf{u}\right)_{\Omega_s,t}, \tag{5}$$

we summarize the gradient computation in the acoustic-elastic coupled FWI into the following three steps: (1) solve the equation system in Eq. (1) to obtain the forward wavefields in both fluid and solid regions, where the required pressure wavefield is computed by $P = -\ddot{\varphi}$; (2) use the same wave propagation engine as in Step (1) to solve the adjoint system in Eq. (3) for the adjoint-wavefield computation in both fluid and solid regions; (3) compute the zero-lag cross-correlation of the forward wavefields and the adjoint wavefields to get the elementary gradients according to Eqs. (4) and (5). The gradient for some other parameters, such as P-wave (V_p) and S-wave (V_s) velocities, can be calculated by the chain rule based on them.

Numerical examples

Here we present two numerical examples using a spectral-element discretization in space, thanks to its easy implementation of boundary conditions and irregular interface.

The first example is based on a simple bilayered 2D model which combines a water layer on the top of a homogeneous solid layer. To illustrate the gradient kernels, we add the perturbation of $+500$ m/s for the P-wave velocity, $+200$ m/s for the S-wave velocity and $+50$ kg/m^3 for the density in the solid layer. A pressure source with 10 Hz Ricker wavelet is applied at the source point for the forward simulation, while the pressure misfit is used as the adjoint source at the receiver point for the adjoint simulation. Figure 1 shows the gradient kernels of P-wave velocity, S-wave velocity and density, which reveals the model parameters can be inferred from the data through the contribution of different waves, such as the diving wave, reflected wave and P-to-S converted wave that supports the S-wave velocity reconstruction.

The second example is the application of acoustic-elastic coupled FWI on a 3D extended Marmousi II model. The V_p and V_s models vary in all three directions and have an uneven seabed (Figures 3a,b). We extract the slices at the seabed, the depth of $z = 0.62$ km and along the crossline direction with $y = 0.42$ km for display. The initial V_p and V_s are smoothed from the true models. We run the acoustic-elastic coupled FWI on three different datasets: (1) pressure data recorded by a towed streamer acquisition with 2 shot lines (38 shots, every 300 m in the inline and crossline directions) and 9 receiver lines for each shot (maximum offset of 5.8 km in the acquisition direction and 225 m in the normal direction), (2) pressure data recorded by a OBC acquisition with 18 shot lines covering the whole $x-y$ plane and 2 ocean-bottom cables (38 4C receivers, every 300 m in the inline and crossline directions), (3) 3C displacement data recorded by the same OBC acquisition as in (2). The source function for all the dataset generation is a 10 Hz Ricker wavelet, and the maximum frequency going to invert is 20 Hz. The inversion process for each dataset is the same, except that a source-receiver reciprocity is applied in the OBC dataset for decreasing the computing cost. The detailed parameter setting and computing cost are listed in Table 1. From the data-fitting illustration in Figure 2, we can find a good agreement between the synthetic data and observed data in all three datasets, implying that a sufficient iteration has been achieved. Thus, the reconstructed results should only be influenced by the dataset itself. Figure 4 shows the reconstructed

Model	Mesh ($x \times y \times z$)	Δt (ms)	NT	Iterations	Data type	Cores	Run time (hour) Band 1	Band 2	Band 3
3D Marmousi II	$102 \times 21 \times 24$	0.55	12,000	60×3	Streamer	1,520	3.85	3.90	4.21
					OBC-P	1,520	3.81	4.12	4.17
					OBC-3C	4,560	3.64	4.02	4.25

Table 1: Summary of parameter setting and computing cost in the acoustic-elastic coupled FWI test. The frequency bands are : $0-5$ Hz (Band 1), $0-10$ Hz (Band 2), $0-20$ Hz (Band 3).

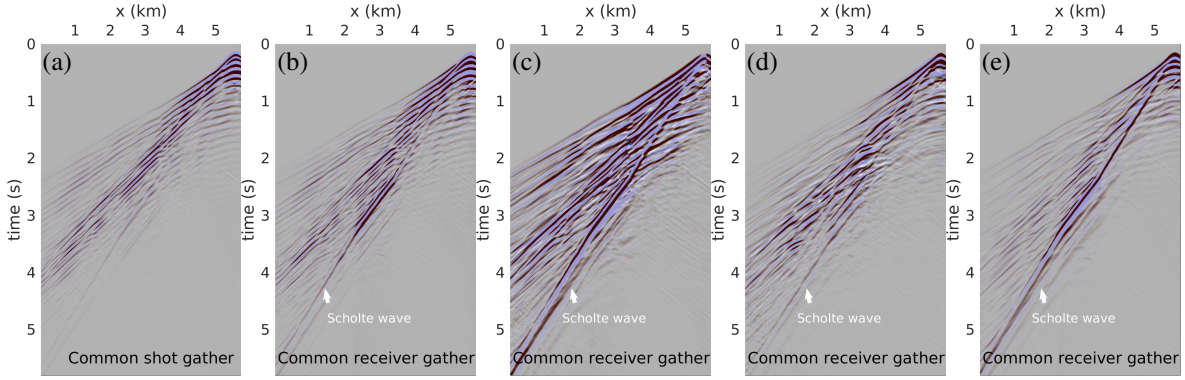

Figure 2: Data fitting in the middle crossline ($y = 0.425$ km) for the pressure data in the streamer acquisition (a), pressure data in the OBC acquisition (b) and 3C displacement data in the OBC acquisition (c: u_x, d: u_y and e: u_z). The synthetic data (plotted in blue-red) are superimposed onto the observed data (plotted in white-black).

models of V_p and V_s in three datasets. As expected, due to a wide-azimuth coverage and long offset, OBC acquisition seems to efficiently mitigate the footprint and unwanted artifacts observed in the streamer acquisition and recovers more structure details in both V_p and V_s (see Figures 4a and 4b). However, a better velocity reconstruction can be seen in the results from 3C displacement dataset (Figures 4c) where the S-wave velocity is almost totally recovered, owing to a direct recording of S-wave at the seabed (see the horizontal components in Figures 2c and 2d).

Conclusions

We proposed an efficient 3D acoustic-elastic coupled FWI engine which can reconstruct jointly P-wave and S-wave velocity models from the multi-component ocean-bottom data. It is developed within the framework of acoustic-elastic coupled wave-equation system, achieving the elastic approximation of the subsurface. Based on the adjoint-state method, the gradient kernels of this acoustic-elastic coupled FWI are constructed using a hybrid approach. It involves two different formulations for representing the acoustic-elastic coupled wave-equation system: the $\varphi - \mathbf{u}_s$ formulation for the forward wavefield computation, and the $P - \mathbf{u}_s$ formulation for the adjoint wavefield computation, which makes it possible to use the same wave propagation engine in the solution of both forward and adjoint problems. The gradient computation based on the bilayered 2D model demonstrates that the possibility of S-wave velocity reconstruction is contributed from the P-to-S converted wave on the seabed. In the case study of 3D extended Marmousi II model, the application of acoustic-elastic coupled FWI to the OBC data reveals a resolution improvement of velocity models, especially for the usage of 3C displacement data.

Acknowledgements

The research leading to these results has received funding from the European Union's Horizon 2020 research and innovation programme under the ENERXICO project, grant agreement No. 828947. This study was also partially funded by the SEISCOPE consortium (`http://seiscope2.osug.fr`), sponsored by AKERBP, CGG, CHEVRON, EQUINOR, EXXON-MOBIL, JGI, SHELL, SINOPEC, SISPROBE and TOTAL. This study was granted access to the HPC resources of CIMENT infrastructure (`https://ciment.ujf-grenoble.fr`), Cray Marketing Partner Network (`https://partners.cray.com`) and CINES/IDRIS/TGCC under the allocation 046091 made by GENCI.

References

Chaljub, E. and Valette, B. [2004] Spectral element modelling of three-dimensional wave propagation in a self-gravitating Earth with an arbitrarily stratified outer core. *Geophysical Journal International*, **158**(1), 131–141.

Maver, K.G. [2011] Ocean bottom seismic: Strategic technology for the oil industry. *First Break*, **29**(12), 75–80.

Peter, D., Komatitsch, D., Luo, Y., Martin, R., Le Goff, N., Casarotti, E., Le Loher, P., Magnoni, F., Liu, Q., Blitz, C., Nissen-Meyer, T., Basini, P. and Tromp, J. [2011] Forward and adjoint simulations of seismic wave propagation on fully unstructured hexahedral meshes. *Geophysical Journal International*, **186**(2), 721–739.

Plessix, R.E. [2006] A review of the adjoint-state method for computing the gradient of a functional with geophysical applications. *Geophysical Journal International*, **167**(2), 495–503.

Virieux, J. and Operto, S. [2009] An overview of full waveform inversion in exploration geophysics. *Geophysics*, **74**(6), WCC1–WCC26.

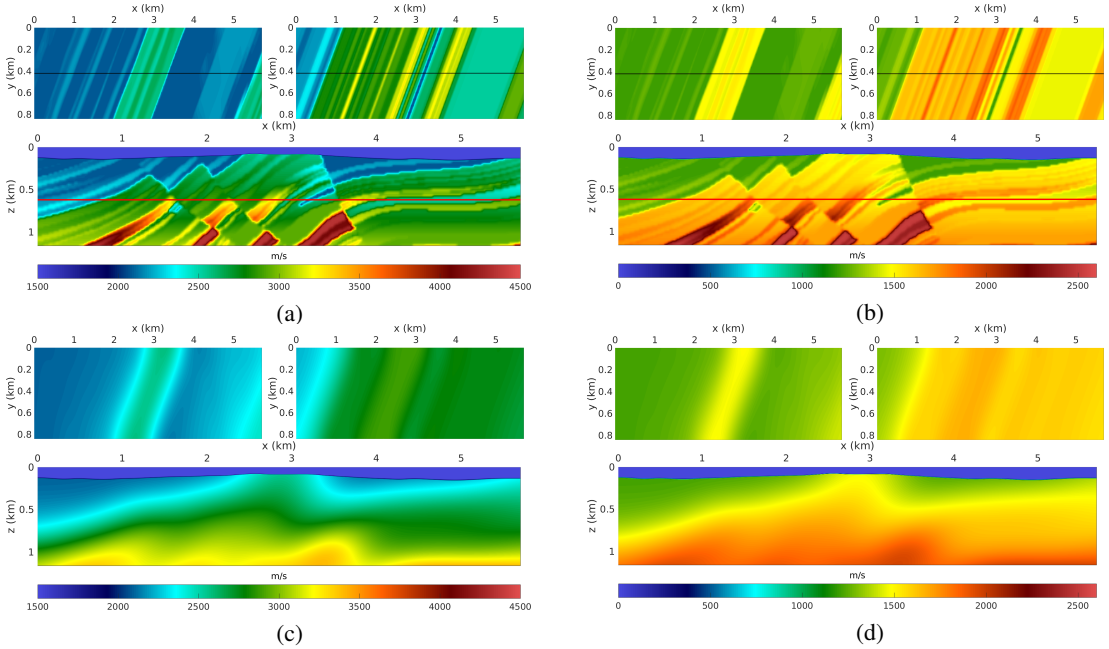

Figure 3: Velocity slices of 3D extended Marmousi II model. True P-wave velocity (a) and S-wave velocity (b). Initial P-wave velocity (c) and S-wave velocity (d). In each figure, the slices at the seabed, $z = 0.62$ km (red line) and $y = 0.42$ km (black line) are shown.

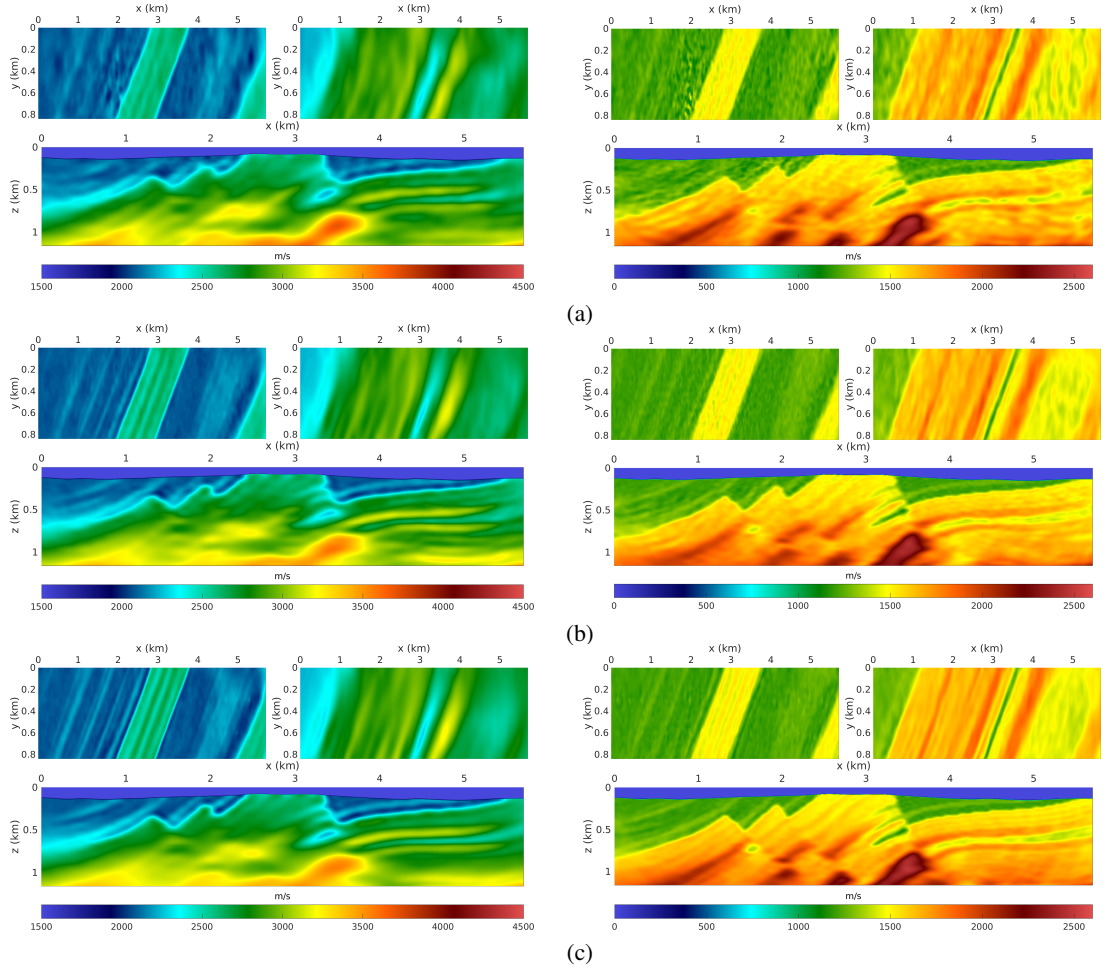

Figure 4: Reconstructed results of P-wave velocity (left column) and S-wave velocity (right column) by using the streamer acquisition (a), OBC acquisition with pressure data only (b) and OBC acquisition with three-component displacement data (c). In each figure, the slices at the seabed, $z = 0.62$ km and $y = 0.42$ km are shown.